



**HAL**  
open science

## From Powdered Oxide to Shaped Metal: an Easy Way to Prepare a Porous Metallic Alloy for SOFC

Dalya Al-Kattan, Pascal Lenormand, Fabrice Mauvy, Patrick Rozier

### ► To cite this version:

Dalya Al-Kattan, Pascal Lenormand, Fabrice Mauvy, Patrick Rozier. From Powdered Oxide to Shaped Metal: an Easy Way to Prepare a Porous Metallic Alloy for SOFC. *Fuel Cells*, 2018, 18 (1), pp.18-26. 10.1002/fuce.201700089 . hal-01728050

**HAL Id: hal-01728050**

**<https://hal.science/hal-01728050>**

Submitted on 30 Oct 2019

**HAL** is a multi-disciplinary open access archive for the deposit and dissemination of scientific research documents, whether they are published or not. The documents may come from teaching and research institutions in France or abroad, or from public or private research centers.

L'archive ouverte pluridisciplinaire **HAL**, est destinée au dépôt et à la diffusion de documents scientifiques de niveau recherche, publiés ou non, émanant des établissements d'enseignement et de recherche français ou étrangers, des laboratoires publics ou privés.






## Open Archive Toulouse Archive Ouverte (OATAO)

OATAO is an open access repository that collects the work of Toulouse researchers and makes it freely available over the web where possible

This is an author's version published in: <http://oatao.univ-toulouse.fr/24516>

**Official URL:** <https://doi.org/10.1002/fuce.201700089>

### To cite this version:

Al-Kattan, Dalya  and Lenormand, Pascal  and Mauvy, Fabrice and Rozier, Patrick  *From Powdered Oxide to Shaped Metal: an Easy Way to Prepare a Porous Metallic Alloy for SOFC.* (2018) *Fuel Cells*, 18 (1). 18-26. ISSN 1615-6846

Any correspondence concerning this service should be sent to the repository administrator: [tech-oatao@listes-diff.inp-toulouse.fr](mailto:tech-oatao@listes-diff.inp-toulouse.fr)

# From Powdered Oxide to Shaped Metal: an Easy Way to Prepare a Porous Metallic Alloy for SOFC

D. Al-Kattan<sup>1</sup>, P. Lenormand<sup>1</sup>, F. Mauvy<sup>2</sup>, P. Rozier<sup>1</sup>\*

<sup>1</sup> CIRIMAT, Université de Toulouse, CNRS, INPT, UPS, 118 route de Narbonne, 31062 Toulouse cedex 9, France

<sup>2</sup> ICMCB, CNRS UPR9048, 87 Avenue du Docteur Schweitzer 33608 PESSAC cedex, France

## Abstract

This work reports a proof of concept to obtain a shaped porous metallic alloy by the reduction at low temperature of an oxide precursor shaped at high temperature. A mixed cations oxide selected for potential applications in solid oxide fuel cells (SOFCs), is prepared using Pechini's polymer route and consolidated using the spark plasma sintering (SPS) technique at temperature in the 900 °C – 1,100 °C range. A pellet of pure AB<sub>2</sub>O<sub>4</sub> spinel-like structure with 10% of open porosity is obtained. The reduction of this pellet under H<sub>2</sub> flow at low temperature (800 °C) allows obtaining a highly porous (48%) metal-

lic pellet which meets all necessary characteristics to be used as mechanical support for the third generation of SOFC (3G-SOFC). The use of oxide precursors widens the accessible temperature range allowing the possibility to stack in one step an oxide precursor of the 3G-SOFC with full densification of the electrolyte. This proof of concept opens the way to the easy and cheap "one step" building of an oxide precursor of 3G-SOFC which will be *in situ* activated during the warming up of the cell.

**Keywords:** 3G-SOFC, Porous Metallic Alloy, Soft Chemistry, Solid Oxide Fuel Cell, Spark Plasma Sintering, Stack Design, Three-Dimensional Porous Support

## 1 Introduction

In the current international context, it made it clear to the world that it's now crucial to develop new ways to produce clean, without harming our environment, renewable and low cost energy. Among the different proposed solutions, solid oxide fuel cells (SOFC) could be an attractive complementary possibility. It is well known that SOFC offer many advantages such as high energy efficiency (above 85%) *via* the combination of the production of heat and electricity, and flexibility in the used fuels (natural gas, hydrogen, biofuels or syngas) through the internal reforming capability of these systems [1, 2]. Nevertheless, one of the drawbacks for the development of this technology is the high working temperature (around 1,000 °C), needed to balance the low ionic conductivity of the best performing active materials rare earth nickelates for the cathode [3], yttria-stabilized zirconia as electrolyte (ZrO<sub>2</sub> – 8% Y<sub>2</sub>O<sub>3</sub>) [4] and nickel/yttria-stabilized zirconia cermet for the anode (Ni-YSZ) [5,6]. Such a high operating temperature induces mechanical stress and more generally degradation of materials thus strongly limiting the life of the cell. To overcome these issues, the challenge is to reduce the working temperature down to at least 800 °C [7]. To reach this objective while main-

taining a high efficiency, a third generation of planar SOFC has been developed. It consists of a thick porous metallic alloy acting as mechanical support of the planar cell on which are deposited the active components with thicknesses ranging from 10 to 50 μm optimized to minimize the overall internal resistance [8–12]. The requirements for efficient shaped porous metal for 3G-SOFC are now well-known and can be summarized as (i) an electronic conductivity of 200 S cm<sup>-1</sup> at the working temperature (800 °C) to ensure the role of current collector, (ii) an interconnected porosity of ca. 40% to enable the diffusion of gaseous species and (iii) a high chemical stability to prevent side reactions with the anode (Ni-YSZ) at the working temperature [13]. The main challenges of such a 3G-SOFC reside in the development of processes allowing assembling, in a single stack, components with different shaping parameters namely, a porous metal usually obtained at low temperature under inert/reducing temperature and a ceramic sintered at high temperature under oxidizing atmosphere. The porous metal support is usually prepared using metallurgy technolo-

[\*] Corresponding author, rozier@chimie.ups-tlse.fr

gies but the deposition of active materials requires the use of successive “physical processes” or “wet routes” in complex multi-step processes. Typical physical processes are atmospheric thermal spraying [14], vacuum spraying [15], powder or suspension spraying [16] while the “wet route” consists in tape casting, screen printing, spray deposition [17] or electrophoretic deposition [18]. The so-called “physical” processes do not require post-deposition heat treatment thus preserving the integrity of the porous metal but they remain expensive for this type of application with a difficult control of the microstructure of the coatings. The “wet route” would achieve acceptable manufacturing costs but a heat treatment at high temperature (1,200 °C – 1,400 °C), necessary to ensure the densification of the electrolyte, is highly detrimental to the mechanical strength and chemical stability of the porous metal [19, 20]. To overcome all the technical issues raised by the currently developed processes, we propose a new and easy route which consists in the preparation at high temperature and in oxidizing atmosphere of a shaped and dense “all-oxide-precursor” of the 3G-SOFC which will be annealed at low temperature (typically working temperature) under reducing atmosphere to generate the metallic parts of the cell while maintaining the integrity of the electrolyte. The use of oxide precursors for both the anode and mechanical support components is expected to allow similar sintering behavior thus enabling the easy shaping and assembling of the “all oxide” half-cell while reaching dense electrolyte. The reduction process, with parameters selected to preserve the integrity of the electrolyte, will generate in a second stage the metallic parts and create open porosity in the anode and mechanical support components. To demonstrate the feasibility of such a strategy we first focus on the mechanical support part using a model composition 70% Fe – 18% Co – 12% Ni (weight ratio) instead of conventionally proposed nickel base superalloy (Hastelloy X) [10] or ferritic steel containing chromium to limit corrosion [11, 12]. Fe and Ni are selected to keep respectively the cost and catalytic activity benefits [21, 22]. Cr is replaced by Co to take advantage of higher  $\text{Co}_3\text{O}_4$  reducibility than  $\text{Cr}_2\text{O}_3$  [23, 24] and to prevent the known poisoning of the electrode related to high Cr diffusion [25]. The temperature, atmosphere and dwell time of the different processes will all be set in relation to the behavior of Ni-YSZ cermet (anode) and YSZ (electrolyte) selected because of their high reported performances [26, 27]. The Spark Plasma Sintering, known as a fast sintering technique [28] and already reported to be efficient in the building of other systems for energy storage [29], will be used to ensure the mastering of the microstructure and to prevent interfacial reactions when assembling the different components of the half-cell. The aim of this report is then to demonstrate the possibility to synthesise a porous metal based mechanical support via the reduction at low temperature (working temperature of 3G-SOFC) of an oxide precursor shaped and consolidated at high temperature (YSZ sintering conditions).

## 2 Experimental Procedure

The oxide precursor is prepared using a chemical process derived from the Pechini’s [30] and Valente [31] routes. Appropriate amounts, to get the 70% Fe – 18% Co – 12% Ni weight ratio, of  $\text{Fe}(\text{NO}_3)_2 \cdot 9\text{H}_2\text{O}$  (Acros Organics, 99.0%),  $\text{Co}(\text{NO}_3)_2 \cdot 6\text{H}_2\text{O}$  (Acros Organics, 99.0%) and  $\text{Ni}(\text{NO}_3)_2 \cdot 6\text{H}_2\text{O}$  (Acros Organics, 99.0%) are dissolved in 10 mL of deionized water to form the “cationic solution” with a total concentration of 0.25 mol  $\text{L}^{-1}$ . Acetylacetone (acac, Sigma-Aldrich 99%) and hexamethylenetetramine (HMTA, Sigma-Aldrich 99%) are selected as chelating agent and polymeric precursor respectively. Equivalent molar amounts of acac and HMTA are dissolved in acetic acid to reach a concentration of 1.88 mol  $\text{L}^{-1}$  defined to be the optimal value insuring homogeneous cation mixing [32, 33]. The cation and organic solutions are mixed together and the total volume is adjusted to 200 mL with acetic acid. The polymerization is obtained after stirring during 30 minutes at 80 °C. The resulting sample is calcined at 450 °C for 7 h to remove the organic components and further annealed at temperatures up to 900 °C to enhance the homogeneity and the crystallinity of the oxide.

The pellets with diameters ranging from 8 mm to 20 mm are prepared using the SPS technique (Dr. Sinter 2080, SPS Syntex Inc., Japan) using a pulsed direct current (pulse duration 3.3 ms). The pulse configuration consists in succession of 12 pulses “on” followed by 2 rests periods. The punches and dies are in graphite and a sheet of graphitic paper is placed between the punches and the die to ensure good electric contact and between the punches and the powder to facilitate the removal of the pellet. The sintering process consists in a fast heating rate (100 °C  $\text{min}^{-1}$ ) up to temperature ranging between 900 °C and 1,200 °C maintained for 1 to 5 minutes. A pressure of 50 MPa is maintained during the sintering process to ensure electrical contact and the whole treatment is conducted in vacuum.

X-ray diffraction (XRD) is performed using a BRUKER AXS D4 Endeavor diffractometer operating in Bragg-Brentano mode ( $\theta$ - $2\theta$ ) with a Cu-K $\alpha$  X-ray source ( $\lambda_{\text{Cu-K}\alpha}$ =0.15418 nm). All scans are collected in the  $2\theta$  range 10° to 100° with an angular step  $2\theta = 0.12^\circ$  and 5.1 s counting time.

Scanning electron microscopy (SEM) is conducted using a JEOL JSM-6700F microscope equipped with a PGT EDS analyzer.

The open porosity is estimated by comparing the density of the pellet determined using the geometric factors (diameter, thickness and weight) and helium based pycnometry using a Micromeritics (AccuPyc 1330) apparatus.

The Temperature-Programmed Reduction (TPR) method, which yields quantitative information on the reducibility of the oxides, is performed using an AutoChem 2920 analyzer and a  $\text{H}_2/\text{Ar}$  (5%–95%) reducing gas mixture. A thermal conductivity detector (TCD) is used to measure the thermal conductivity of the gas which is then converted into concentration of active gas.

The electrical properties of the samples are determined using the 4 probes technique in the temperature range 20 °C–800 °C with 2 °C min<sup>-1</sup> heating and cooling rates. Electrical contacts are ensured by platinum wires sealed with a platinum paste.

### 3 Results and Discussion

#### 3.1 Powdered Oxide Precursor Synthesis and Characterization

Oxide based compounds with weight ratio 70:18:12 in Fe-Co-Ni respectively have been prepared following the process described in the experimental section. The XRD patterns of the samples annealed at temperature ranging from 450 °C to 900 °C are reported in the Figure 1 together with SEM pictures of samples annealed at 450 °C and 900 °C. The comparison of the XRD pattern with database shows that the sample obtained at 450 °C is characteristic of a mixture of AB<sub>2</sub>O<sub>4</sub> spinel-like structure and M<sub>2</sub>O<sub>3</sub> corundum-like structure which is maintained after annealing at increasing temperature up to 900 °C. The increase of the annealing temperature induces a sharpening of the Bragg peaks indicating the growing of the particles. This growing is confirmed by SEM investigation which shows an increase of the particle size from 0.1 μm at 450 °C up to 1 μm at 900 °C. To prevent the growth of particles known to be detrimental to obtain a homogeneous shaping of the oxide precursor, we decided to determine the behavior of this mixture of oxide without trying to reach single phase material. The reducibility of the powdered oxide precursor is determined using the Temperature Programmed Reduction technique on the sample annealed at 900 °C which presents the largest particle size, i.e., the worst condition for the reduction. The sample is heated up to 900 °C in a constant flow of a 95–5 Ar-H<sub>2</sub> gas mixture. The reduction process is characterized by the evolution of the thermal conductivity of the gas which, directly related to the amount of H<sub>2</sub>, allows determining the H<sub>2</sub> consumption versus temperature. The evolution reported in the Figure 2a shows the existence of a broad peak between 350 °C and 600 °C characteristic of the consumption of H<sub>2</sub> corresponding to the reduction process. The broadness indicates that the reduction occurs in different stages in agreement with the two-phase character of the oxide precursor. Nevertheless, the reduction is completed at 600 °C, a temperature largely below the working temperature of the 3G-SOFC targeted between 700 °C and 800 °C. Based on these results and to be as close as possible to the 3G-SOFC working conditions, a powdered oxide precursor sample is heat treated in pure H<sub>2</sub> flow at 800 °C for 2 h. The examination of the XRD pattern collected on the as-obtained sample (Figure 2b) shows that all Bragg peaks can be indexed using a single Face Centred Cubic structural model. FCC model being typical for iron based alloys it indicates that despite the oxide precursor is a mixture, a homogeneous alloy is obtained. The SEM picture reported in the Figure 2c shows that the average particle

size is around 1 μm so that the combination of the reduction process, expected to decrease the particle size (removal of oxygen), and high temperature treatment, expected to increase the particle size, balance each other thus limiting the microstructure evolution from the oxide precursor to the metallic alloy. EDS analysis (Figure 2d) shows that the different elements are homogeneously distributed in the whole sample which confirms the formation of a metallic alloy rather than a mixture of metallic compounds.

#### 3.2 Shaping of the Oxide Precursor and Characterization of the Pellets

The Spark Plasma Sintering technique is well-known to allow fast heat treatment processes leading to the control of both microstructure and densification from consolidation to full sintering [28]. It has already proved to be efficient in building, in one step, stack of different components with good mechanical properties via the mastering of interfacial reactions allowing localised interpenetration while preventing full reaction [29]. For all these advantages, this technique is selected for the shaping of the oxide precursor with the aim of obtaining a pellet with open and connected porosity in a ratio high enough to allow, for the reduction stage, diffusion of H<sub>2</sub>. A first test is made using soft conditions selected to ensure the consolidation of the sample without sintering. These conditions, schematically reported in insert of Figure 3, correspond to a heating rate of 100 °C min<sup>-1</sup> up to 900 °C maintained during 1 min. A pressure of 50 MPa, the lowest value needed to

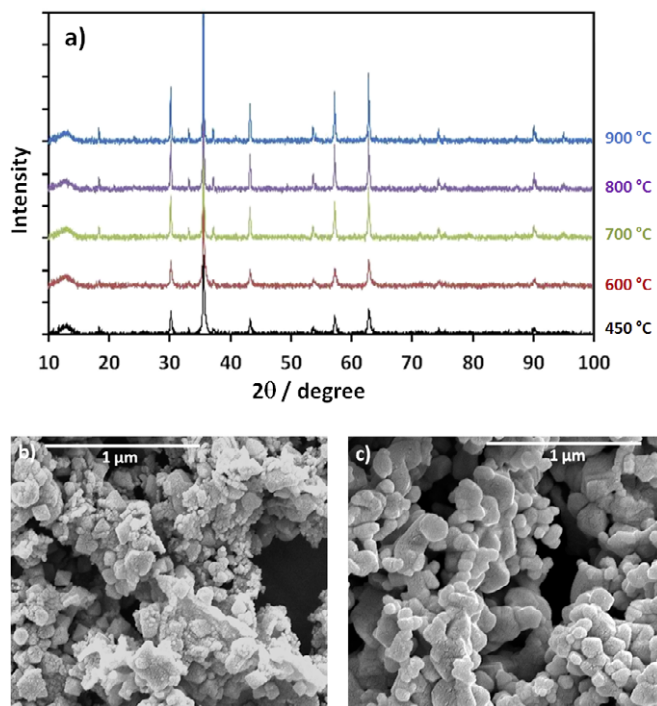


Fig. 1 (a) XRD patterns collected at room temperature on mixed precursor oxide powders annealed at various temperatures, SEM analysis obtained on powders treated at (b) 450 °C and (c) 900 °C.

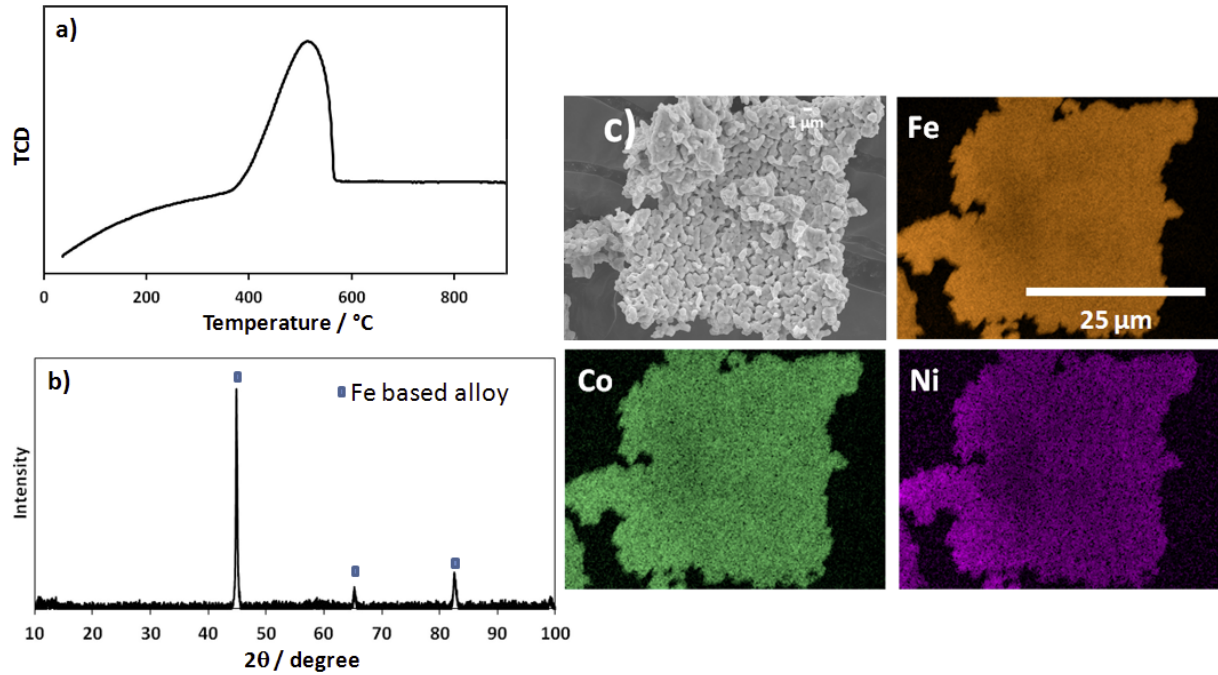


Fig. 2 (a) TPR measurement on mixed precursor oxide powder annealed at 800 °C, (b) XRD patterns (c) SEM and (d) EDS analysis of the sample after reducing treatment at 800 °C under pure H<sub>2</sub>.

ensure the electrical contact, is applied during the whole process. The displacement of the punch, automatically adjusted to maintain a constant pressure, is used as a gauge of the evolution of the sintering process. Its evolution versus temperature, reported in the Figure 3, shows that the consolidation process occurs between 550 °C and 700 °C and that there is no extra sintering phenomena up to 900 °C. The pellets recovered after the SPS treatment are annealed for 2 h in air at 700 °C to remove the residual carbon. The XRD pattern collected on the surface of the pellet is reported in the Figure 4a. It has to be

noted that the low resolution of the pattern is typical of samples obtained using SPS where the direct contact of the surface with the punches, acting as current collector, induces local perturbation of the long range ordering of the sample. The SEM picture reported in the Figure 4b confirms this specificity showing the presence, at the surface of the pellet, of acicular particles with 10 μm length and 0.1 μm diameter. The XRD pattern (Figure 4a) can then be indexed using a single AB<sub>2</sub>O<sub>4</sub> spinel-like structural model indicating that even though the disappearance of the M<sub>2</sub>O<sub>3</sub> phase cannot be clearly confirmed,

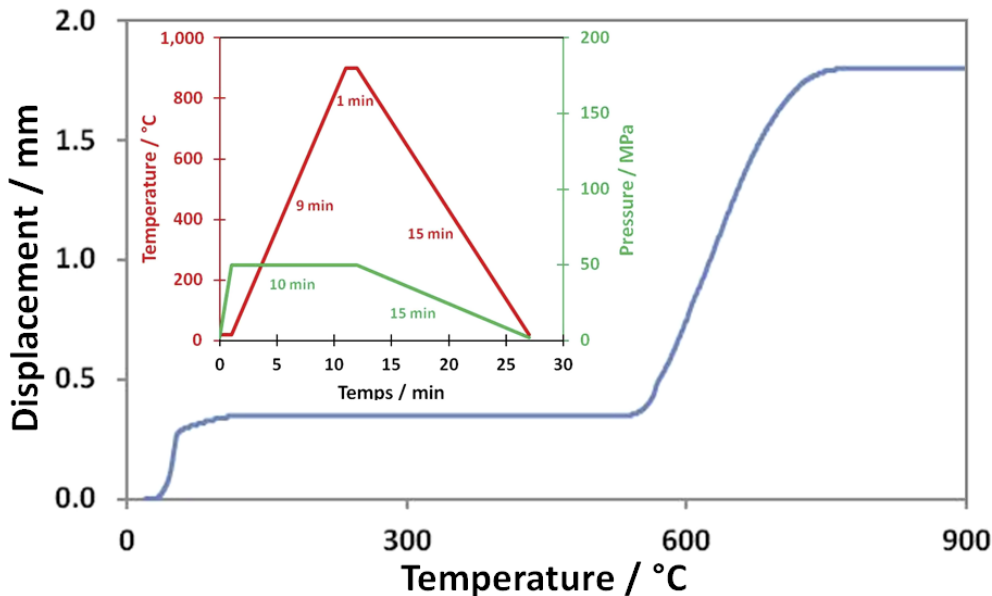


Fig. 3 Typical sintering curve obtain during the SPS treatment. In insert, the SPS conditions applied (temperature profile and pressure) are reported.

the SPS process seems to induce a reactive sintering process enhancing the homogeneity of the oxide precursor. This specific effect is in agreement with already reported results showing the benefit of SPS in synthesizing highly refractive compounds in shorter times than using conventional solid state routes [34]. At this stage it should be underlined the main difference between SPS treatment of a homogeneous mixture and of a stack of components. The former case leads to full reaction due to the high amount of interfaces between the different reactants which allows considering SPS treatment as a reactive sintering. In the latter case, the control of temperature and dwell time allows governing the interfacial reactions localised in between the two components of a stack, thus enabling the assembly while preventing full reaction [35]. Then the benefit of SPS to enhance the homogeneity of the mixed oxide is absolutely not opposed to the limitation of the reaction between the different components of the targeted stack. In both cases, due to the short time of the process, the reaction is limited to the interfaces but induces full reaction in case of a homogeneous mixture of components (a lot of interfaces) and is restricted to a short thickness in case of a stack. The comparison of the density of the sample determined from the geometry of the pellet and using He based pycnometer (Table 1) shows that, while the consolidation of the sample is obtained, 10% of open porosity is maintained after the SPS treatment which is suitable to ensure the diffusion of gas through the whole pellet during the reduction process.

The preparation of an “all oxide precursor” of the full 3G-SOFC implies, during the shaping stage, to ensure the full densification of the electrolyte component. As the shaping and assembling of the oxide precursors is expected to be the only high temperature heat treatment of the full process, SPS conditions should be adapted to match the densification of the electrolyte suppress component while maintaining some porosity in the oxide precursor of the metallic alloys. The densification

of YSZ, the most conventional electrolyte used, occurring at temperature above 1,200 °C, the behavior of the mixed oxide has been investigated at temperature ranging from 900 °C up to 1,200 °C while keeping a pressure of 50 MPa and dwell time of 1 minute. A first experiment at 1,200 °C shows, during the SPS process, the presence of metallic droplets appearing between the dies and the punches. Analysis of the obtained sample confirms the partial reduction of the mixed oxide,

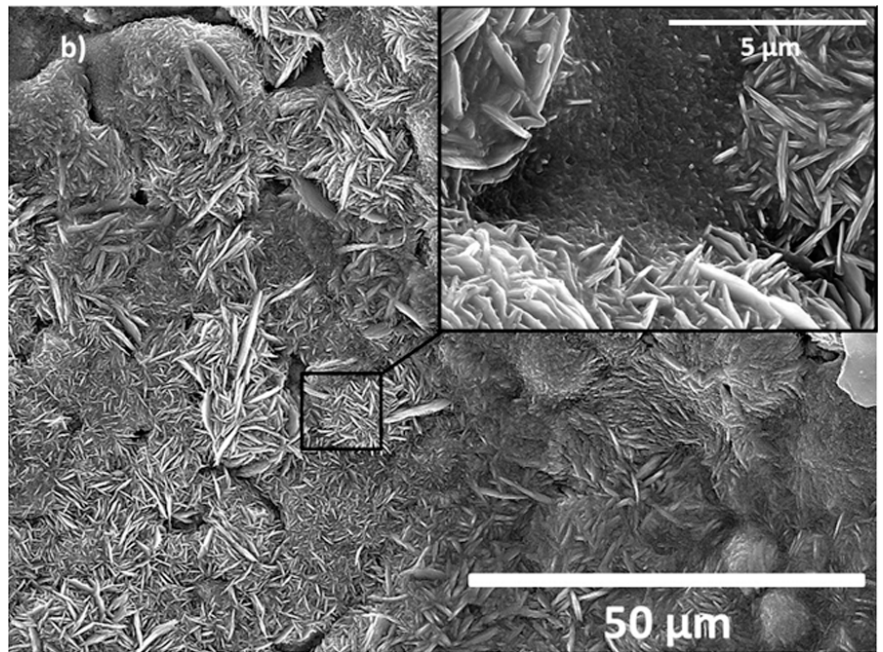
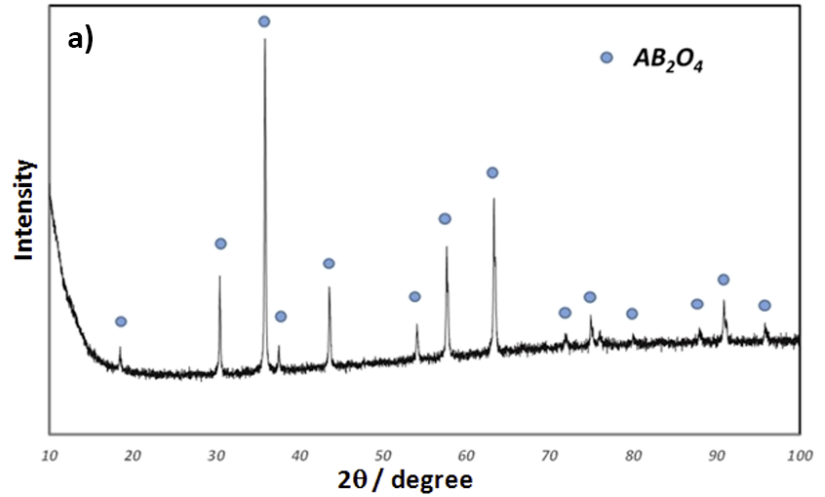


Fig. 4 (a) XRD patterns obtained at room temperature and (b) SEM analysis of the precursor oxide pellet after SPS treatment at 900 °C.

Table 1 Determination of the density of the pellets before and after reducing treatment (theoretical, macroscopic and by He pycnometry) and evaluation of the open porosity.

	Thickness / mm	Diameter / mm	$\rho_{\text{macroscopic}} / \text{g cm}^{-3}$	$\rho_{\text{theoretical}} / \text{g cm}^{-3}$	$\rho_{\text{pycnometer}} / \text{g cm}^{-3}$	Porosity / %
Oxide precursor	2.20 (1)	8.34 (1)	4.60 (1)	5.26	5.19 (1)	11
Reduced sample	1.96 (1)	8.31 (1)	4.11 (1)	8.05	7.90(1)	48

probably due to the reducing surrounding resulting from the combination of vacuum and contact with graphite. To prevent this phenomenon, the temperature is reduced down to 1,100°C and the dwell time increased up to 5 minutes while keeping the same pressure (50 MPa). The XRD pattern collected on the surface of the as obtained pellet (Figure 5a) shows that the whole pattern can be indexed using  $AB_2O_4$  spinel-like structure. The sharpening of the Bragg peaks compared to the one characteristic of pellets sintered at 900°C can be attributed to the growing of particles in agreement with the higher temperature. The SEM investigation confirms the presence of the acicular particles at the surface of the pellet (Figure 5b) while the bulk part of the pellet shows the presence of spherical particles with size around 1  $\mu\text{m}$  (Figure 5c). These differences in morphology between the surface and the core are related, as explained above, to the specificity of the SPS technique and not to the presence of a second phase as confirmed by the XRD investigation (Figure 5a). The open porosity is evaluated close to 11% showing that, despite the increase of the temperature, the use of short dwell time and low pressure prevent the full densification of the sample.

### 3.3 Reducing Process and Porous Metallic Alloy Characterization

The reducing parameters have been selected to be representative of the operating condition of 3G-SOFC. The pellets of the oxide precursor obtained following different sintering procedures have been heated at 800°C in pure  $H_2$  for 2 h. After

this treatment pellets with metallic shine aspect and mechanical behavior good enough to allow easy handling are recovered. The XRD pattern, reported in the Figure 6a, can be indexed, similarly to the reduced powdered sample, using an iron FCC structure model and no Bragg peaks of pristine oxide can be detected showing that the reduction occurred on the whole sample. The cell parameters have been refined using the profile matching method [36] implemented in the FULLPROOVE I.L.L. program [37]. The refined value equals to 3.55 Å is in agreement with the 3.57 Å calculated one using the Vegard's law taking into account the substitution of Co and Ni to Fe. Then, it can be concluded that even using SPS parameters adapted to obtain a dense electrolyte, the oxide precursor can be consolidated while maintaining an open porosity large enough to ensure the reduction down to the metallic state. Moreover, despite a drastic structure change from the oxide to the metal the cohesion of the pellet is maintained.

The comparison of the size of the pellet after  $H_2$  treatment with the one of the pristine oxide precursor shows that the macroscopic shrinkage of the pellet remains limited (11%) and highly anisotropic with a quasi constant diameter of the pellet. This evolution is in perfect agreement with the increase of the open porosity from 11% to 48% (Table 1), as evaluated using the method previously described. The SEM investigation on a cross-section of the reduced pellet shows spherical particles with average size around 0.1  $\mu\text{m}$  connected to each other to form a 3D network including a large porous volume in agreement with the 48% experimentally determined (Figure 6c).

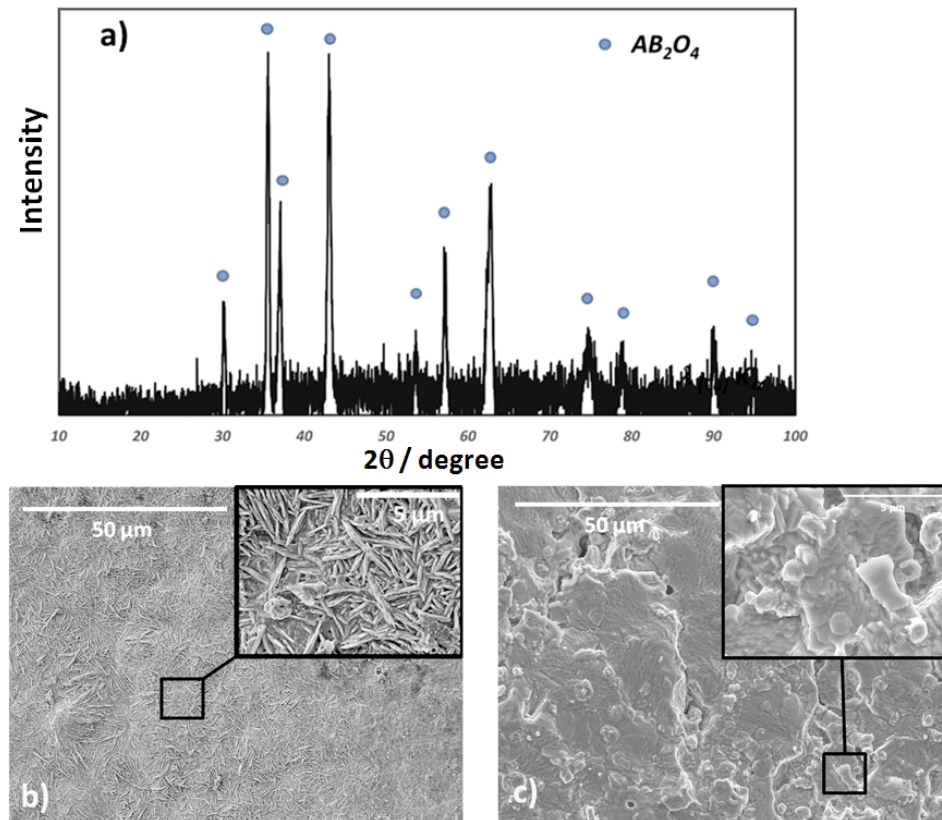


Fig.5 (a) XRD patterns obtained at room temperature on precursor oxide pellet after SPS treatment at 1,100°C and the corresponding SEM analysis of the pellet, top-view (b) and cross section view (c).



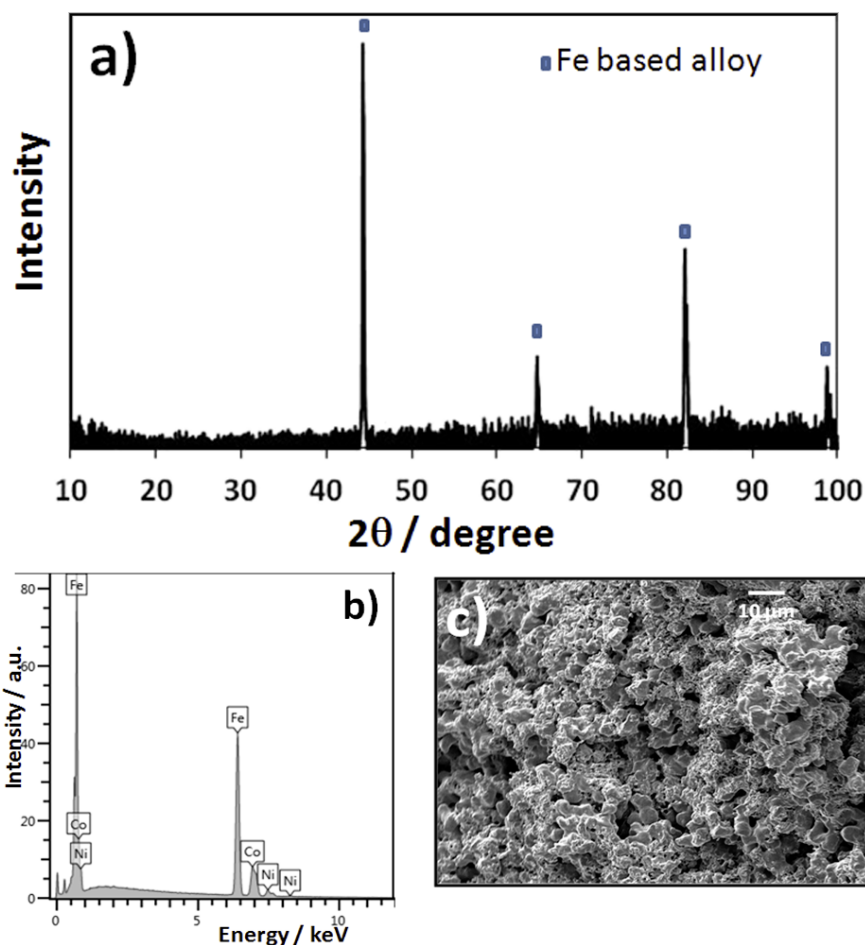


Fig. 6 (a) XRD patterns obtained at room temperature (b) EDS analysis and (c) SEM investigation of the pellet shaped by SPS at 1,100 °C and reduced under pure H<sub>2</sub> at 800 °C for 2 h.

Then, in an unexpected way, the reduction of the pellet of the oxide precursor allows a large increase of the open porosity without destruction of the pellet. The comparison of the theoretical density of the obtained alloy and pristine oxide precursor (respectively 8.05 and 5.26 g cm<sup>-3</sup>) shows that the reduction process induces a large contraction at the grain scale. This is confirmed by the evolution of the particle size from 1 μm (oxide) down to 0.1 μm (metal) observed with SEM experiments. However, this volume change is balanced by an increase of the open porosity from 10% to around 50% while maintaining the contact between the particles. The temperature of the reduction process appears then to be low enough to prevent any sintering of the pellet while maintaining the cohesion of the sample.

Successive annealing up to 800 °C in both neutral (Ar) and reducing (H<sub>2</sub>) atmospheres didn't lead to any changes in the pellet morphology neither than microstructure showing the stability of the as obtained metallic alloy. The Coefficient of Thermal Expansion determined in Ar atmosphere leads to a value  $\alpha = 12 \cdot 10^{-6} \text{ K}^{-1}$  close to the one reported for the other targeted components ( $\alpha = 10.5 \cdot 10^{-6} \text{ K}^{-1}$  for YSZ) and falling in the 10 to 12  $\cdot 10^{-6} \text{ K}^{-1}$  range usually reported for the selection of SOFC materials. The electrical properties of the samples have

been investigated using the conventional four probes technique. Two pellets obtained using the same batch of the oxide precursor have been prepared using the same SPS parameters ( $T = 1,100 \text{ °C}$ ; dwell = 1 min;  $P = 50 \text{ MPa}$ ). They have been annealed in air at 700 °C for 12 h to remove remaining carbon. One pellet has been reduced under pure H<sub>2</sub> flow at 800 °C for 2 h while the second one is kept in the oxide state. The structural and microstructural characterization of the pellets shows that they are similar to the one described in the previous part. The "oxide" pellet presents an open porosity around 10% and the reduced one corresponds to a metallic alloy and shows an open porosity around 45%. The measurement of the electrical conductivity is carried out in a H<sub>2</sub> atmosphere in the temperature range 20 °C–800 °C. The data characteristics of the first heating are not collected as they correspond to the homogenisation of the samples. The Figure 7 reports the data measured during the first cooling from 800 °C down to room temperature and the full second cycle for both samples. It can be seen that both samples exhibit the same behavior with a decrease of the conductivity with increasing temperature typical of a metallic behavior. The conductivity determined at 800 °C (the targeted working temperature of the

3G-SOFC) is 400 and 600 S cm<sup>-1</sup> respectively, matching reported requirements. Moreover, both samples exhibiting the

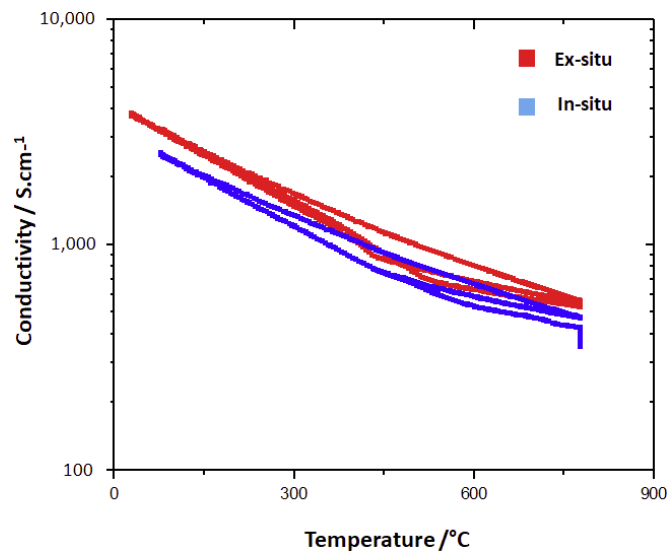


Fig. 7 Electrical conductivity versus temperature of pellets reduced ex situ and in situ measured in the temperature range (room temperature RT– 800 °C) under controlled atmosphere (Ar/H<sub>2</sub> 95%/5%).

same behavior, it can be deduced that the “oxide-precursor” pellet has been fully *in situ* reduced during the initial heating stage in H<sub>2</sub> leading to sample similar to the one obtained by *ex situ* reduction at 800 °C during 2 h. This indicates that the microstructure of the “oxide-precursor” with only 10% of open porosity insures a complete reduction even in short time and shows that once the full oxide based 3G-SOFC will have been obtained, the pre-treatment under H<sub>2</sub> will not be needed. Moreover, the absence of drastic evolution along cycling indicates the stability of the pellet versus successive heating and cooling.

The combination of the investigations carried out on both the shaped oxide-precursor and reduced metallic alloy shows that the proposed new way of designing porous metal acting as mechanical support in 3G-SOFC is promising. The requirements already reported in terms of electrical properties, open porosity and mechanical strength are all satisfied. The comparison with reported values for metallic support obtained using conventional metallurgy techniques does not evidences any drawbacks from the proposed two stages process. The oxide-precursor pellet is reduced down to the metal state even in conditions corresponding to the warm up of the SOFC (heating up to 800 °C without dwell time). The obtained sample is characteristic of an alloy with homogeneous composition and an open porosity around 48%. The reduction process allows preserving the pellet as the loss of oxygen is balanced by the increase of the open porosity, while a good contact between the metallic particles is maintained. This is perfectly confirmed by the electrical measurements indicating that a conductivity as high as 400 S cm<sup>-1</sup> is obtained. The CTE is also perfectly adapted to the requirement as it falls in the reported admissible range and should guarantee a good behavior when in contact with the other components. One has to note in addition, that preliminary tests (reported in a forth coming paper) have been performed to stack the “oxide-precursor” half SOFC cell (mechanical support/NiO-YSZ/YSZ) using the same process. The optimization of the parameters leads after the reduction process to a typical porous metal/porous Ni-YSZ cermet/dense YSZ half cell with characteristics matching the requirements and close to the one obtained using the complex multi steps processes conventionally used.

## 4 Conclusion

The reported works aim at proposing a new strategy allowing obtaining a 3G-SOFC using a simple two stages process. The shaping and assembly of an “all oxide precursor” of the cell at high temperature is followed, in a second stage, by low temperature heat treatment in reducing atmosphere to generate the metallic parts. This first study consists in the evaluation of the potentiality of this approach to obtain a porous metal that can act as mechanical support of the cell. The targeted composition of the metallic alloy has been selected to keep the low cost advantage of Fe, the performing catalytic activity of Ni while Co is chosen to limit corrosion. The powdered oxide

precursor is prepared using soft chemistry route to enhance the homogeneous distribution of the elements, and SPS fast sintering process is selected to obtain the pellet while mastering the microstructure. As expected, this oxide precursor can be shaped and consolidated using conditions (temperature; duration) identical to the one needed to obtain fully dense electrolyte. The open porosity of the as-obtained pellet, despite low (10%), is high enough to ensure the complete reduction of the sample in conditions identical to the working conditions of 3G-SOFC. The operating temperature is high enough to ensure the full reduction of the sample, as confirmed by the obtained single phased alloy, and low enough to prevent the shrinkage of the pellet, as confirmed by the large increase of the open porosity (48%). In addition, the heat treatment allows maintaining the cohesion of the sample *via* a perfect tuning of the connection between the grains as confirmed by the measured electronic conductivity largely above requested one for 3G-SOFC. This study clearly confirms the benefit of the “oxide precursor concept” which allows the shaping of an oxide precursor of the mechanical support without heat treatment restriction. This enables the possibility to use this oxide precursor as mechanical support for the deposition of all the active components and to adapt, without restriction, post heat treatments to ensure densification and assembly. The efficiency of the reduction process will generate in a second stage, that can occurs during the warming up of the 3G-SOFC, the open porosity and metallic components with limited size variation of the pellet and preservation of the dense electrolyte. The use of soft chemistry route to prepare the oxide precursor allows in addition to tune the chemical composition of the different components especially the one of the metallic support to meet all the requirements in terms of corrosion or diffusion of elements for examples. The suppression of the antagonism between needed porous metal and dense ceramic on both sides of a same stack opens the way to the easy design of “all oxide precursor of 3G-SOFC” without restriction on the composition of the other components neither than on the deposition process used.

## Acknowledgement

The authors would like to acknowledge S. Secou (ICPEES – University of Strasbourg, France) and G. Chevallier (PNF2-CNRS – University of Toulouse, France) for their experimental assistance and the many fruitful discussions.

## References

- [1] C. Zuo, M. Liu, *Solid Oxide Fuel Cells*, Springer, New York, USA, 2012, pp. 7–35.
- [2] B. Timurkutluk, C. Timurkutluk, M. D. Mat, Y. Kaplan, *Renewable and Sustainable Energy Reviews* 2016, 56, 1101.
- [3] H. Zhao, F. Mauvy, C. Lalanne, *Solid State Ionics* 2008, 179, 35.
- [4] J. W. Fergus, *J. Power Sources* 2006, 162, 30.

- [5] W. Z. Zhu, S. C. Deevi, *Mater. Sci. Eng. A* **2003**, 362, 228.
- [6] J. Kong, K. Sun, D. Zhou, N. Zhang, J. Mu, J. Qiao, *J. Power Sources* **2007**, 166, 337.
- [7] Z. Wang, J. O. Berghaus, S. Yick, C. Decès-Petit, W. Qu, R. Hui, R. Maric, D. Ghosh, *J. Power Sources* **2008**, 176, 90.
- [8] I. Villarreal, C. Jacobson, A. Leming, Y. Matus, S. Visco, L. De Jonghe, *Electrochem. Solid-State Letter* **2003**, 6, A178.
- [9] T.-L. Wen, D. Wang, M. Chen, H. Tu, Z. Lu, Z. Zhang, H. Nie, W. Huang, *Solid State Ionics* **2002**, 148, 513.
- [10] J. W. Fergus, *Mater. Sci. Eng. A* **2005**, 397, 271.
- [11] W. J. Quadackers, H. Greiner, W. Köck, *Proc. 1<sup>st</sup> European Solid Oxide Fuel Cell Forum*, Lucerne, Switzerland, **1994**, 525.
- [12] W. J. Quadackers, J. Piron-Abellan, V. Shemet, L. Singheiser, *Mater. High. Temp.* **2003**, 20, 115.
- [13] Y. Yan, R. Bateni, J. Harris, O. Kesler, *Surface & Coatings Technology* **2015**, 272, 415.
- [14] S. Takenoiri, N. Kadokawa, K. Koseki, *J. Therm. Spray. Technol.* **2000**, 9, 360.
- [15] R. Vassen, D. Hathiramani, J. Mertens, *Surf. Coat. Technol.* **2007**, 202, 499.
- [16] K. A. Khor, L. G. Yu, S. H. Chan, X. J. Chen, *J. Eur. Ceram. Soc.* **2003**, 23, 1855.
- [17] J. H. Joo, G. M. Choi, *J. Power Sources* **2008**, 182, 589.
- [18] Y. B. Matus, L. C. De Jonghe, C. P. Jacobson, S. J. Visco, *Solid State Ionics* **2005**, 176, 443.
- [19] N. P. Brandon, D. Corcoran, *J. Mater. Eng. Perform.* **2004**, 13, 253.
- [20] M. Lang, P. Szabo, Z. Ilhan, *J. Fuel Cell Science Tech.* **2007**, 4, 384.
- [21] R. Sachitanand, M. Sattari, J. E. Svensson, J. Froitzheim, *Int. J. Hydrogen Energy* **2013**, 38, 15328.
- [22] J. G. Grolig, J. Froitzheim, J. E. Svensson, *J. Power Sources* **2014**, 248, 1007.
- [23] H. Y. Lin, Y. W. Chen, *Mater. Chem. Phys.* **2004**, 85, 171.
- [24] T. Li, R. J. Brook, B. Derby, *J. Eur. Ceram. Soc.* **1999**, 19, 399.
- [25] G. Jalilvand, M. A. Faghihi-Sani, *Int. J. Hydrogen Energy* **2013**, 38, 12007.
- [26] M. Han, X. Tang, H. Yin, S. Peng, *J. Power Sources* **2007**, 165, 757.
- [27] R. J. Gorte, J. M. Vohs, *Curr. Opin. Colloid Interface Sci.* **2009**, 14, 236.
- [28] R. Orrù, R. Licheri, A. M. Locci, A. Cincotti, G. Cao, *Materials Science and Engineering* **2009**, 63, 127.
- [29] G. Delaizir, V. Viallet, A. Aboulaich, R. Bouchet, L. Tortet, V. Seznec, M. Morcrette, J.-M. Tarascon, P. Rozier, M. Dollé, *Adv. Funct. Mater.* **2012**, 22, 2140.
- [30] M. P. Pechini, N. Adams, *US Patent US 3330697*, **1967**.
- [31] I. Valente, *PhD Thesis*, University of Pierre et Marie Curie Paris VI, Paris, France, **1989**.
- [32] P. Lenormand, S. Castillo, J. R. Gonzalez, C. Laberty-Robert, F. Ansart, *Solid State Sciences* **2005**, 7, 159.
- [33] M. Fontaine, C. Laberty-Robert, A. Barnabé, F. Ansart, P. Tailhades, *Ceram. Int.* **2004**, 30, 2087.
- [34] E. Dumont-Botto, C. Bourbon, S. Patoux, P. Rozier, M. Dollé, *J. Power Sources* **2011**, 196, 2274.
- [35] J. Galy, M. Dollé, T. Hungria, P. Rozier, J. P. Monchoux, *Solid State Sciences* **2008**, 10 (8), 976.
- [36] H. M. Rietveld, *J. Appl. Crystallogr.* **1969**, 2, 65.
- [37] J. Rodriguez-Carjaval, "FULLPROF" I.L.L. program, Grenoble, France, **1992**.